Excited state potential energy surfaces of N -phenylpyrrole upon twisting: reference values and comparison between BSE/GW and TD-DFT

Iryna Knysh, Kelvine Letellier, Ivan Duchemin, Xavier Blase, Denis Jacquemin

Excited state potential energy surfaces of N-phenylpyrrole upon twisting: Reference values and comparison between BSE/*GW* and TD-DFT

Iryna Knysh,[1] Kelvine Letellier,[1] Ivan Duchemin,[2] Xavier Blase,[3] and Denis Jacquemin[1,4]

[1)]*Nantes Université, CNRS, CEISAM UMR 6230, F-44000 Nantes, France*

[2)]*Univ. Grenoble Alpes, CEA, IRIG-MEM-L_Sim, 38054 Grenoble, France*

[3)]*Univ. Grenoble Alpes, CNRS, Institut Néel, F-38042 Grenoble, France*

[4)]*Institut Universitaire de France (IUF), F-75005 Paris, France*

The puzzling case of the mixing between the charge transfer (CT) and local excited (LE) characters upon twisting of the geometry of N-Phenylpyrrole (N-PP) is investigated considering the six low-lying singlet excited states (ES). The theoretical calculations of the potential energy surfaces (PES) have been performed for these states using a Coupled Cluster method accounting for the impact of the contributions from the triples, many-body Green's function *GW* and Bethe-Salpeter equation (BSE) formalisms, as well as Time-Dependent Density Functional Theory (TD-DFT) using various exchange-correlation functionals. Our findings confirm that the BSE formalism is more reliable than TD-DFT for closely-lying ES with mixed CT/LE nature. More specifically, BSE/GW yields a more accurate evolution of the excited state PES than TD-DFT when compared to the reference coupled cluster values. BSE/*GW* PES curves also show negligible exchange-correlation functional starting point dependency in sharp contrast with their TD-DFT's counterparts.

I. INTRODUCTION

The discovery of dual fluorescence in 4-(dimethylamino)benzonitrile (DMABN)[1] resulted in extensive studies of other compounds that may exhibit similar photophysics. Indeed, the interest in dual emission is coming from a variety of applications where the relative fluorescence intensities and lifetimes of the two bands can be tuned as a function of the conditions (analyte sensing). In addition, dual emission can also lead to a brightness increase or an improvement of the photostability of dyes.[2–6] The push-pull molecules showing dual emission are usually characterized by one "normal" emission band in a non-polar medium and the appearance of a second "abnormal" redshifted band in polar solvents, the latter having an intensity proportional to the polarity of the medium. Since the discovery of dual fluorescence, there were numerous debates in the photophysics and photochemistry communities and several different mechanisms have been proposed to rationalize the experimental observations.[7–12] Nowadays, the widely accepted explanation is given by the twisted intramolecular charge transfer (TICT) model.[6,7,12] This mechanism was first proposed by Grabowski *et al.* in 1973[7] and, according to it, the appearance of the "abnormal" fluorescence band occurs after twisting of the dialkylamino group at 90° with respect to the aromatic ring in the excited state (ES) leading to conformation referred to as the "TICT state".

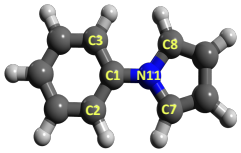

FIG. 1. Structure of the N-PP molecule and numbering of the atoms defining the key twist angle.

N-Phenylpyrrole (N-PP) is an example of a flexible push-pull molecule, with a pyrrole donor (D) and phenyl acceptor (A) (see Figure 1), that possesses valuable photophysical properties such as i) a dual emission from two relaxed singlet states; ii) the possibility to tune absorption and fluorescence bands positions by substitution; and iii) large dipole moments.[13,14] Thereby it was the subject to both experimental and theoretical investigations.[14–20] As can be seen in Figure 2 the absorption process is slightly different in N-PP and DMABN. In the case of N-PP the absorption band is assigned to the transition from the ground state (GS) to the second excited state (S_2) which contrasts with DMABN for which the excitation occurs between GS and the first ES (S_1). This is due to the large oscillator strength of these transitions and the relatively low one of the S_1 excitation in N-PP.[18,20] Experimentally, this results in an energetically higher absorption peak for N-PP (ca. 4.86 eV in n-heptane) than DMABN (cA. 4.05 eV in cyclohexane).[15,21] After being

excited to the S_2 state N-PP undergoes internal conversion to the S_1 state. Eventually, this state undergoes geometrical relaxation yielding a first minimum, which has a local excited (LE) state character. This is the structure to which the "normal" fluorescence band is assigned. According to experiment this is the only band present in the emission spectra measured in non-polar solvents, with a maximum at ca. 4.08 eV (n-heptane and n-hexane).[15,22] In polar media, the appearance of the additional "abnormal" emission band is explained by lowering the energy of the S_3 state (which has a CT nature) due to rotation of the pyrrole ring, acting here as a substituted amino donor, yielding the TICT geometry. Such movements are possible in polar solvents only as a consequence of the large dipole moment of this CT state and the vibronic interactions with the medium that strongly stabilize this state. Moreover, Yoshihara *et al.*[22] reported dipole moments for LE (μ_{LE}) and CT (μ_{CT}) states of N-PP derived from solvatochromic and thermochromic solvent shifts of the fluorescence. According to their findings μ_{LE} is around -3.0 or 1.6 D, while μ_{CT} is ca. 13 D. Even though the accuracy of such dipole moment measurements remains an open question, these results show that the dipole moment of the state generating the "abnormal" fluorescence band of N-PP is large.

Another interesting fact about N-PP is the presence of two low-lying CT states (S_3 and S_4) in the planar conformation, while four CT states can be found after twisting to 90°.[23] This is the reason why this molecule is included in numerous training sets for the studies of CT transition energies.[16,18,20,23–27] However, in contrast to DMABN there is, to the best of our knowledge, only one work reporting the ES potential energy surfaces (PES) of N-PP.[18] However, this work studied one ES PES upon the twisting only and uses the CASPT2/6-31G(d) level of theory. It is important, especially in the case of TICT molecules, to look at the evolution upon twisting of several ES PES to confirm the fluorescence mechanisms. Moreover, the PES shapes constitute a stringent test for quantum chemistry methods.[28] In our previous work[29] we studied the PES of the two lowest excited states of DMABN and compared the Coupled Cluster (CC), Time-Dependent Density Functional Theory (TD-DFT), and many-body Green's function (*GW*) - Bethe-Salpeter equation (BSE) descriptions. Our results showed that BSE/*GW* outperformed TD-DFT both quantitatively and qualitatively for the description of the PES of both states. The reason for the success of the former method lies in the underlying theory. The BSE formalism[30–37] uses the corrected quasiparticle energies obtained with the *GW* many-body approach,[38–41] which is based on many-body Green's function (*G*) perturbation theory to lowest order in the screened Coulomb potential (*W*). The main advantage of the BSE/*GW* scheme as compared to TD-DFT, with which it shares the same compu-

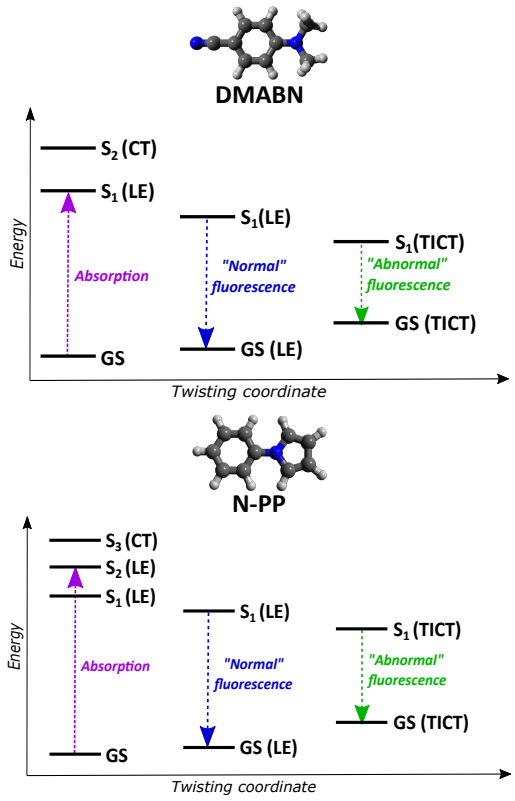

FIG. 2. Comparison of photophysics behind dual fluorescence of DMABN and N-PP. The "abnormal" fluorescence band appears only in polar solvents, while the "normal" fluorescence band is present in both polar and non-polar media as well as in the gas phase.

tational scaling, is the correct description of the nonlocal electron-hole interactions that results in an accurate prediction of the energies of CT states.[42–48] Moreover, the BSE/*GW* formalism can be made much less dependent from the starting XCF than TD-DFT when using the so-called partially self-consistent scheme (ev*GW*), where the molecular orbital coefficients (eigenvectors) remain conserved but the eigenvalues are self-consistently obtained.[49,50] This scheme was found to be efficient in removing the differences brought by DFT functionals for the transition energies.[46,51] However, a significant weak spot of BSE/*GW*, as compared to TD-DFT, is the lack of analytical gradients, which in contrast are available since many years in TD-DFT thanks to the so-called *Z*-vector approach.[52–54] Together with an early investigation of the retinal chromophore,[55] our previous work on DMABN[29] was the first to explore the quality of the ES PES for medium size molecules at BSE/ev*GW* level, whereas only small molecules were reported before at this level of theory,[56–58] including with approximate ES analytic forces.[56] However, our DMABN study was limited to two states of different spatial symmetries.

In this work, we go further and target the description of the six lowest ES PES of N-PP upon the twisting of the angle between the benzene ring and pyrrole moiety. This is more challenging than DMABN since, on the one hand, more closely-lying states are present and, on the other hand, significant mixing of LE and CT characters occurs during the twisting, which is usually harder to reproduce. This work is also aiming at providing the first high-level references for the ES PES of N-PP which are used to assess the performance of both TD-DFT and BSE/GW methods for their PES.

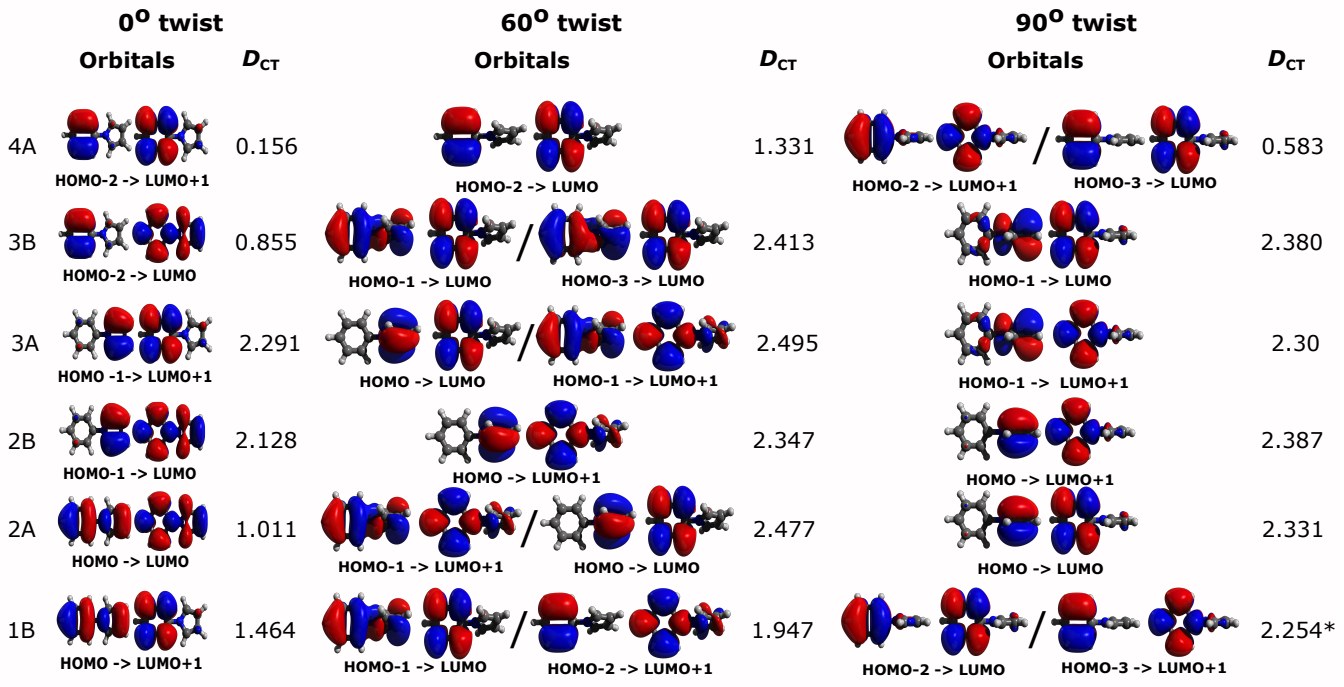

FIG. 3. Hartree-Fock molecular orbitals participating in the excitation of the six lowest excited states determined from CCSD(T)(a)*/cc-pVTZ calculations and the corresponding D_{CT} parameters calculated at TD-CAM-B3LYP/cc-pVTZ level of theory for the 0°, 60°, and 90° structures. The molecular orbitals have been drawn with a contour threshold of 0.02 au. The states are ordered from the lowest (bottom) to the highest (top) total energy as predicted for the untwisted structure by the CCSD(T)(a)*/cc-pVTZ level of theory. * This D_{CT} is impacted by the mixing between the closely-lying 1B and 2B states at the TD-CAM-B3LYP/cc-pVTZ level.

II. COMPUTATIONAL DETAILS

The set of ground state (GS) geometries of N-PP was obtained by rotation of the pyrrole ring around the single bond with phenyl ring from 0° to 90° by 10° step. To this end, we constrained the twist angles (C3-C1-N11-C8 and C2-C1-N11-C7, see Figure 1) while the rest of the molecule was allowed to relax. These constrained geometries were optimized at the CCSD/cc-pVDZ level of theory leading to C_{2v} symmetry for the 0° and 90° geometries and C_2 symmetry for the intermediate conformations. The geometry optimizations were performed with a *tight* convergence criterion, using the Gaussian 16 program.[59] Cartesian coordinates are given in the ESI†.

The ES calculations have been done using the CC, TD-DFT, and BSE/*GW* formalisms systematically applying the cc-pVTZ atomic basis set, considering the six lowest singlet ES. More specifically, at the CC level we used second-order Coupled Cluster (CC2)[60–63] within the resolution of identity (RI) approximation as coded in the Turbomole package,[64] as well as CCSD[65–69] and CCSD(T)(a)* (with pertubative triples)[70] as implemented in the CFOUR2.1 program.[71] The latter predicts highly accurate transition energies, typically within 0.05 eV of full CI.[72] TD-DFT calculations have been achieved with the following exchange-correlation functionals (XCF): PBE,[73] PBE0,[73,74] and CAM-B3LYP[75]. These computations have been done with the aid of the Gaussian 16 program and do not use the Tamm-Dancoff approximation (TDA). BSE/ev*GW* results have been obtained starting from the above listed XCF using the BEDEFT package,[76–78] an extension of the FIESTA code,[51,79,80] where the input Kohn-Sham eigenstates were obtained from the ORCA 5.0 program.[81] The 10 highest occupied and the 10 lowest unoccupied eigenvalues were corrected at the ev*GW* level. The susceptibility operators and the optical excitations for BSE/ev*GW* calculations were constructed from all occupied/virtual states. The energy dependence of the self-energy is treated exactly using a recently improved analytic continuation scheme.[76] The Coulomb-fitting resolution of the identity[82] was used with the cc-pVTZ-RI auxiliary basis set. TDA was not applied during the BSE calculations.[81,83,84] Additionally, Le Bahers' CT distance (D_{CT}) parameter[85,86] was calculated at the TD-CAM-B3LYP/cc-pVTZ level of theory using the Gaussian 16 program.

In the analysis of the data we use the relative energy term (ΔE_{rel}) which is calculated as a difference between the total energy of the ES (E_{ES}) and the GS energy of the planar structure ($E_{\mathrm{GS}}^{0^\circ}$):

$$\Delta E_{\mathrm{rel}} = E_{\mathrm{tot}} - E_{\mathrm{GS}}^{0^\circ}$$

where for the BSE approach we use the GS energies provided by DFT. Additionally, we also

determine the difference in relative energies for different methods ($\Delta E_{\text{diff}}^{\text{Method}}$) compared to the reference CCSD(T)(a)* data:

$$\Delta E_{\text{diff}}^{\text{Method}} = \Delta E_{\text{rel}}^{\text{Method}} - \Delta E_{\text{rel}}^{\text{CCSD(T)(a)*}}.$$

III. RESULTS AND DISCUSSION

We start by discussing the molecular orbitals (MO) participating in the excitation of the six lowest-lying ES (Figure 3). Let us start by discussing the "simple" 2A state in the two extreme twist angles. Interestingly, this state can be mainly ascribed to a HOMO-LUMO transition both at 0° and 90°, yet its nature differs at these two geometries. In the planar conformation, both frontier orbitals are delocalized over the full molecule, and the transition has a $\pi \rightarrow \pi^{\star}$ character. The D_{CT} amplitude (calculated with the TD-CAM-B3LYP/cc-pVTZ method) is small, ca. 1 Å, typical of local excitation. In contrast, in the orthogonal conformation, the HOMO is located in the pyrrole and the LUMO on the benzene, the 2A state having now a clear CT character with a D_{CT} exceeding 2 Å. Besides, in N-PP, in contrast to DMABN,[29] one notices two CT states for the planar structure, that is, the 2B and 3A states (S_3 and S_4, at CCSD(T)(a)*/cc-pVTZ level of theory). This can be seen from the orbitals that participate in these transitions as well as from the D_{CT} amplitude (calculated with the TD-CAM-B3LYP/cc-pVTZ method) that exceeds 2 Å for these two states only in the planar conformation. Upon a 60° twisting, one can spot a few changes to the orbitals and the D_{CT} values of all ES. First, all the states experience an increase in CT character which means that the states presenting a LE nature at the untwisted structure become mixed, *i.e.*, have a fraction of CT character. Second, significant mixing of orbital contributions is seen for all states, except 2B and 4A, with two competitive orbital sets needed to describe the transition. Finally, at 90° one clearly sees four CT states with electronically decoupled donor and acceptor units (as stated above 2A, but also 2B, 3A, and 3B), where the CT transition occurs from the pyrrole ring to the orthogonal benzene one. Although the 1B state seems to be a LE state according to the MO charge distribution, its D_{CT} is rather high, hinting at the presence of a partial CT character here as well (see below). We wish to mention a few points before entering into the discussion of the PES. As can be seen in Figure 3, the MO participating in the transition of the 2A and 3A states at the twisted geometry are reversed. This arises from the fact that, upon twisting, these two states come close to each other. At 60° twist, it is hard to follow the states by their orbital contributions. That is why for these states we follow the smooth energy evolution path and

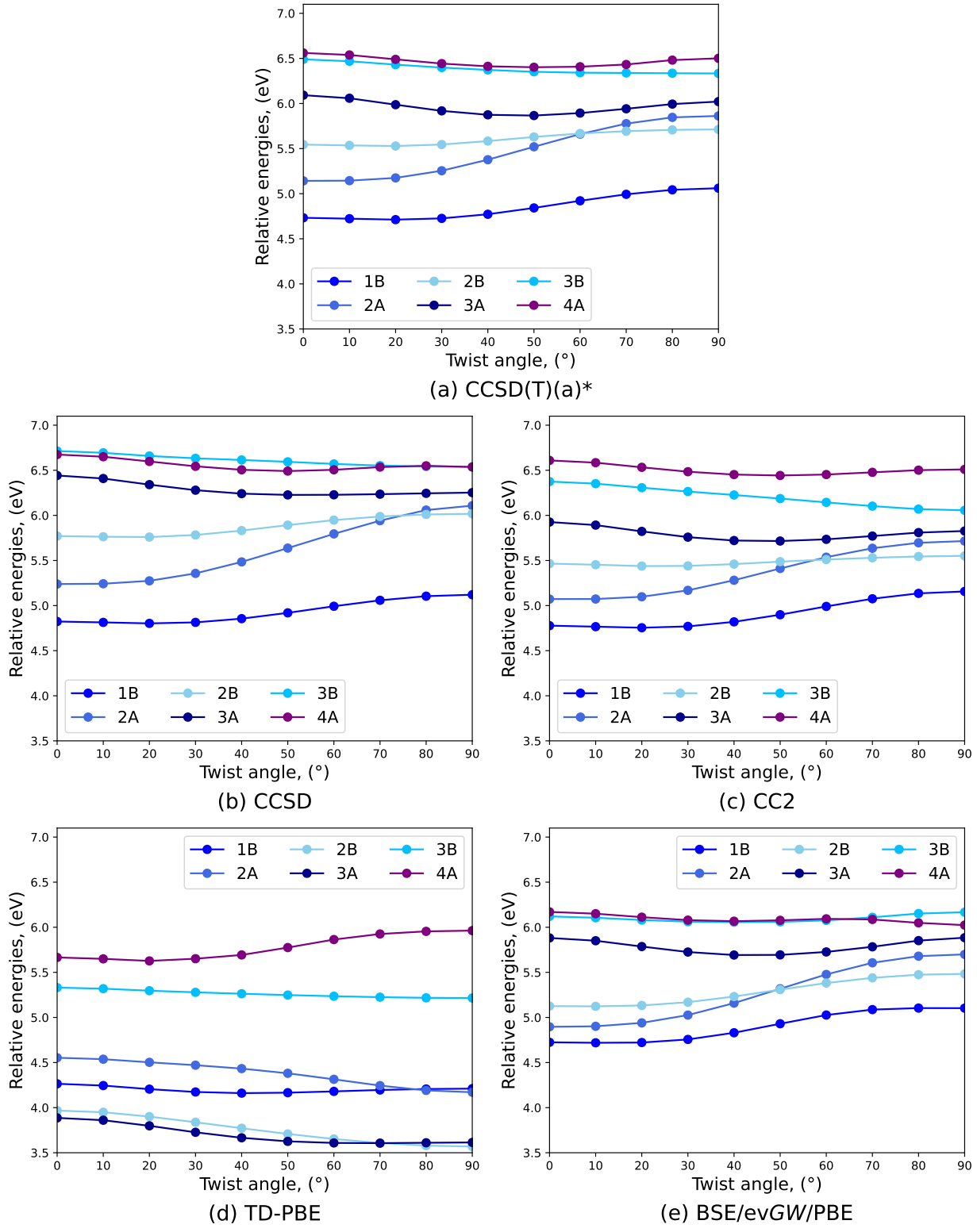

FIG. 4. Six lowest ES PES of N-PP obtained with the (a) CCSD(T)(a)*, (b) CCSD, (c) CC2, (d) TD-PBE, and (e) BSE/ev*GW*/PBE levels of theory using the cc-pVTZ atomic basis set. The GS energy of the planar structure is used as a reference for the calculation of relative energies (BSE/ev*GW*/PBE uses PBE ground state energy).

we keep the orbitals occupation as presented in Figure 3. We underline that this 2A/3A mixing occurs for all electronic structure methods used in this work. Additionally, a similar problem arises with TD-CAM-B3LYP, which leads to an exchange of the orbitals between 1B and 2B states at 80-90° twist, because these two states are energetically closer with TD-CAM-B3LYP than with other levels of theory (see Figure S1). In this case, we also follow the smooth energy evolution rather than orbitals participation in these two states. We present only the Hartree-Fock (HF) orbital contributions in Figure 3, but the topologies of the DFT MO are highly similar. Furthermore, for all studied methods, we could identify the ES with the same orbital contribution as for CCSD(T)(a)*, although in some cases the ordering of the states differs (see the discussion below).

The PES of the six low-lying ES of N-PP along the twisting coordinate are presented in Figure 4. CCSD(T)(a)* stands as the highest level of theory used in this work and is our "gold standard" for testing the other methods. The curves displayed in Figure 4a for this method show several interesting features: i) a single crossing between the 2A and 2B ES taking place at 60°; ii) smooth increase (decrease) of the energy along the twisting coordinate for 2A (3B); iii) more complex evolution for the other four ES that all show a minimum; and iv) nearly degenerated 3B and 4A states, but at very large twist angles. Even though the global PES topologies are roughly similar at all CC levels, one can notice significant differences between these methods, which was not the case for the DMABN:[29] i) the crossing between the 2A and 2B states takes place at the same angle for both CC2 and CCSD(T)(a)* (60°), while for CCSD it is shifted to a higher value (*ca.* 75°); ii) at the twisted orthogonal geometry, the 1B and 2B states are closer to each other at the CC2 level, and much more separated at the CCSD level than at the reference level; iii) the two highest states, namely 3B and 4A, swap ordering upon twisting with CCSD, an effect not seen with CCSD(T)(a)*, while with CC2 the gap between these states is strongly exaggerated, even though the ordering is preserved. Additionally, we provide the relative energies for these methods as well as the differences with the reference one and mean absolute errors (MAE) in the ESI† (Tables S1-S7). One notices that CC2 provides more accurate energies than CCSD for all states studied (see also Figure S2). There are reports about the CCSD trend to overestimate the transition energies as compared to higher levels techniques.[72,87,88]

We now analyze the TD-DFT results obtained within the generalized gradient approximation (GGA, here PBE which has 0% of exact exchange). We can clearly see that the PES are collapsed: the ordering of the states is wrong, there are more crossings between the states than with CCSD(T)(a)*, and only the two last states have the right ordering, though they are too separated

from one another. This is not a surprise that TD-PBE is performing badly in this case, since it is known to break down for the ES having a CT character. This misbehavior is due to the wrong description of the nonlocal electron-hole interactions, that are only captured by the (insufficient) quarter of *exact* exchange present in PBE0.[28] N-PP is clearly a more difficult case than DMABN due to a larger number of CT states. In contrast, BSE/ev*GW* starting from PBE eigenstates is still performing very well, resulting in the correct evolution of the excited state surfaces upon twisting. However, BSE tends to underestimate the relative energies as compared to CCSD(T)(a)*. We also provide graphs for both methods using one global hybrid (PBE0) and one range-separated hybrid (CAM-B3LYP) in the ESI† (see Figure S3). Looking at those graphs, one can see that TD-DFT is very functional-dependent and only CAM-B3LYP restores the good evolution of the N-PP PES, which was expected, since this range-separated hybrid functional includes an increasing ratio of *exact* exchange when the interelectronic distance increases, up to 65% at long range, which allows to correctly capture (most of the) electron-hole interactions at large separation.[28,29] On the other hand, the BSE formalism is able to keep almost perfectly independent from the starting point, but for a few small differences, *i.e.*, BSE/ev*GW*/PBE0 and BSE/ev*GW*/CAM-B3LYP shift the crossing point between 2A and 2B states closer to 60° (as in the reference CCSD(T)(a)* data) and also swap the 3B and 4A ordering as compared to the BSE/ev*GW*/PBE. However, this does not strongly impact the accuracy of the calculations as the difference between the MAE values for the three BSE schemes is less than 0.15 eV (see Tables S15-S21 in the ESI†).

In addition to the PES evolution, it is also interesting to compare the predicted barriers to cross during the twisting in order to reach the TICT geometry. In the gas phase as in non-polar solvents, one does not observe the emission from the TICT state,[15] and thus the energetic barrier to reach this state should be significant. This is well reproduced by all levels, except the TD-PBE and TD-PBE0 methods which deliver the wrong trends for the PES. We provide in Table I the crossing barrier (ΔE_{cross}) for all tested methods, except for both TD-PBE and TD-PBE0 that are dismissed for their inaccuracy. At the CC level, CC2 predicts a crossing barrier consistent with CCSD(T)(a)* (0.46 and 0.52 eV, respectively), whereas CCSD is overestimating the reference value by 0.24 eV. On the other hand, TD-CAM-B3LYP yields the opposite trend and predicts more than twice lower ΔE_{cross} than CCSD(T)(a)*. Notably, BSE/ev*GW* crossing barriers are in the good range irrespective of the starting point, with BSE/ev*GW*/CAM-B3LYP exactly matching the reference ϕ_{cross} crossing angle and ΔE_{cross} barrier.

Finally, we take a closer look at the evolution of the differences in relative energies (ΔE_{diff})

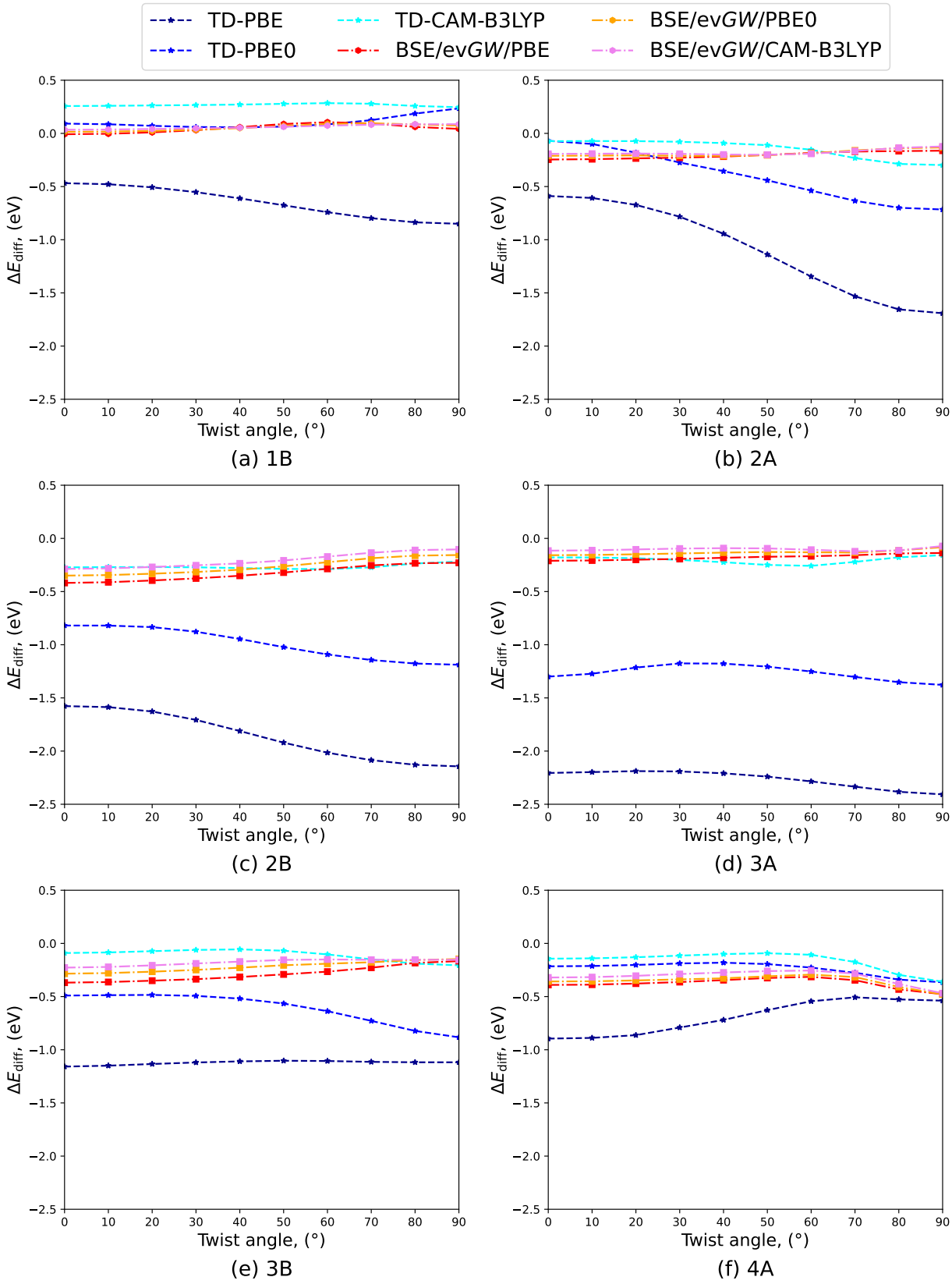

FIG. 5. The differences (ΔE_{diff}) between relative energies obtained with TD-DFT and BSE/ev*GW* methods using PBE, PBE0, and CAM-B3LYP XCF compared to the CCSD(T)(a)* reference for the (a) 1B, (b) 2A, (c) 2B, (d) 3A, (e) 3B, and (f) 4A states of N-PP. See the Computational details section for more information.

TABLE I. Crossing angle between the 2A and 2B states (ϕ_{cross}) and related crossing barrier (ΔE_{cross}) given by the CC, TD-DFT, and BSE/ev*GW* methods.

Method	ϕ_{cross}, (°)	ΔE_{cross}, eV
CCSD(T)(a)*	60.0	0.52
CCSD	75.0[b]	0.76
CC2	60.0	0.46
TD-CAM-B3LYP	40.0	0.22
BSE/ev*GW*/PBE	50.0	0.42
BSE/ev*GW*/PBE0	55.0[b]	0.46
BSE/ev*GW*/CAM-B3LYP	60.0	0.52

[a] $\Delta E_{\text{cross}} = E(\phi_{\text{cross}}) - E(\phi_{0^\circ})$.

[b] These are approximated angles (see Figures 4 and S3) and the total ES energies at these angles were approximated from average of the vicinal angles.

upon the twist between the TD-DFT and BSE/ev*GW* results (with PBE, PBE0, and CAM-B3LYP) and the reference CCSD(T)(a)* method for each state of N-PP studied (Figure 5). The relative energies as well as the ΔE_{diff} values can be found in ESI† (Tables S8-S21). Additionally, we also show the comparison between the above-mentioned methods for each ES PES of N-PP in Figure S4. We know from the analysis of orbital contributions and D_{CT} amplitudes that the 1B state has a LE nature at low twist angle and gains some CT character at larger distortions. That is why we can see a big contrast between TD-PBE and the reference which increases upon the twist. On the other hand, TD-PBE0 yields almost zero values of ΔE_{diff} until the 70° twist. TD-CAM-B3LYP is known to be able to improve the description of the CT state, but has been reported to have a tendency to overestimate the LE state energies of low-lying states of large conjugated molecules.[89] In contrast, BSE with all XCF provides very accurate surfaces (ΔE_{diff} close to zero, see Figure 5a) with negligible starting point dependency. As can be seen in Figure 5, the next four states are quite challenging for both TD-PBE and TD-PBE0 due to their significant CT character, especially at large twist angles. Interestingly, TD-CAM-B3LYP shows an increase of the ΔE_{diff} upon twisting, while BSE/ev*GW* (with all three functionals) yields almost flat curves for the 2A state. However, for the next two states, 2B and 3A, these methods deliver similar results. For the two remaining

states (3B and 4A), TD-CAM-B3LYP yields a better agreement with the reference values, but the energetic differences with the reference increase at large twist angles. The BSE formalism does not perform better as the energies show a rather inaccurate evolution in this case as well (see also Figure S4) which results in quite high values of ΔE_{diff}. We reported a similar behavior for BSE/ev*GW* in our previous study of DMABN[29] and concluded that it was related to the DFT GS energy. Finally, comparing the relative TD-DFT and BSE/ev*GW* energies to CCSD(T)(a)* (Tables S8-S21), one notices that for half of the states, TD-CAM-B3LYP delivers lower MAE values (1A, 2B, and 4A states), while for the other half, BSE/ev*GW*/CAM-B3LYP is more accurate (1B, 2B and 3A states). Although the total MAE values given in Tables S14 and S21 are very close for those two methods, as can be seen in Figure 5 BSE approach usually provides more uniform ΔE_{diff} than TD-DFT. Indeed the BSE errors are skewed by the large MAE obtained for the highest-lying (4A) state. Overall, the significant advantage of BSE/ev*GW* formalism lies in the more accurate evolution of the surfaces with negligible starting point dependency, in sharp contrast with TD-DFT.

CONCLUSIONS

In the present contribution, we studied the evolution of the six lowest ES of N-PP during the twist of the pyrrole ring. Three coupled cluster methods, as well as both TD-DFT and BSE/ev*GW* combined with different XCF have been assessed. We report here the first highly accurate [CCSD(T)(a)*/cc-pVTZ quality] PES for N-PP that we could use to benchmark all the other levels of theory. The N-PP is a more complicated molecule than the often treated DMABN due to closely-lying ES with CT character and even at the CC level we observed small differences when climbing the CC ladder. Interestingly, CC2 predicts ES energies closer to the CCSD(T)(a)* ones than CCSD. Our results also show that the BSE formalism can accurately reproduce the evolution of closely-lying excited states PES as well as correctly predict the crossing barrier during the twist. Even if TD-CAM-B3LYP is able to restore accurate trends for the evolution of the PES upon twisting, it fails to provide a good estimate of the crossing barrier. Furthermore, the BSE/ev*GW* approach gives results almost independent from the starting XCF, which was known for energies but only very recently demonstrated for PES. Overall, the BSE/ev*GW* approach is a valuable alternative to TD-DFT in the case of complicated LE/CT mixed states. We are currently working on further developments aiming at computing more efficiently ES properties with BSE/ev*GW*. Knowing the BSE/ev*GW* oscillator strengths are accurate,[90] we plan to move to more

complex properties. In the light of previous studies[91] assessing the merits of other strategies, such as non-self-consistent BSE/G_0W_0 starting from an optimally-tuned functional, may also stand as an additional path to validating BSE PES.

CONFLICTS OF INTEREST

There are no conflicts to declare.

ACKNOWLEDGEMENTS

The authors are indebted to the French Agence Nationale de la Recherche (ANR) under contract ANR-20-CE29-0005 (BSE-Forces) for financial support. K.L. is indebted to the EUR LUMOMAT program and the Investments for the Future program (contract ANR-18-EURE-0012) for their support. The authors are thankful for the generous allocations of time by the CCIPL computational center installed in Nantes and by the national HPC facilities (contract GENCI-TGCC A0110910016).

REFERENCES

[1]E. Lippert, W. Ludar, and H. Boss, *Advances in Molecular Spectroscopy* (Pergamon Press, Oxford, 1962).

[2]M. Ren, B. Deng, X. Kong, K. Zhou, K. Liu, G. Xu, and W. Lin, Chem. Commun. **52**, 6415 (2016).

[3]S. Yu, X. Yang, Z. Shao, Y. Feng, X. Xi, R. Shao, Q. Guo, and X. Meng, Sens. Actuators B Chem. **235**, 362 (2016).

[4]Y. Zhang, J. Zhang, J. Shen, J. Sun, K. Wang, Z. Xie, H. Gao, and B. Zou, Adv. Opt. Mater. **6**, 1800956 (2018).

[5]L. Meng, S. Jiang, M. Song, F. Yan, W. Zhang, B. Xu, and W. Tian, ACS Appl. Mater. Interfaces **12**, 26842 (2020).

[6]C. Wang, W. Chi, Q. Qiao, D. Tan, Z. Xu, and X. Liu, Chem. Soc. Rev. **50**, 12656 (2021).

[7]K. Rotkiewicz, K. Grellmann, and Z. Grabowski, Chem. Phys. Lett. **19**, 315 (1973).

[8]W. Schuddeboom, S. A. Jonker, J. M. Warman, U. Leinhos, W. Kuehnle, and K. A. Zachariasse, J. Phys. Chem. **96**, 10809 (1992).

[9]K. A. Zachariasse, T. von der Haar, A. Hebecker, U. Leinhos, and W. Kuhnle, Pure Appl. Chem. **65**, 1745 (1993).

[10]S. I. Druzhinin, N. P. Ernsting, S. A. Kovalenko, L. P. Lustres, T. A. Senyushkina, and K. A. Zachariasse, J. Phys. Chem. A **110**, 2955 (2006).

[11]A. L. Sobolewski and W. Domcke, Chem. Phys. Lett. **259**, 119 (1996).

[12]Z. R. Grabowski, K. Rotkiewicz, and W. Rettig, Chem. Rev. **103**, 3899 (2003).

[13]S. Murali and W. Rettig, J. Phys. Chem. A **110**, 28 (2006).

[14]A. Neubauer, J. Bendig, and W. Rettig, Chem. Phys. **358**, 235 (2009).

[15]A. Sarkar and S. Chakravorti, Chem. Phys. Lett. **235**, 195 (1995).

[16]B. Proppe, M. Merchán, and L. Serrano-Andrés, J. Phys. Chem. A **104**, 1608 (2000).

[17]S. I. Druzhinin, V. A. Galievsky, T. Yoshihara, and K. A. Zachariasse, J. Phys. Chem. A **110**, 12760 (2006).

[18]X. Xu, Z. Cao, and Q. Zhang, J. Phys. Chem. A **110**, 1740 (2006).

[19]S. I. Druzhinin, S. A. Kovalenko, T. A. Senyushkina, A. Demeter, R. Machinek, M. Noltemeyer, and K. A. Zachariasse, J. Phys. Chem. A **112**, 8238 (2008).

[20]I. Fdez. Galván, M. E. Martín, A. Muñoz-Losa, M. L. Sánchez, and M. A. Aguilar, J. Chem. Theory Comput. **7**, 1850 (2011).

[21]I. Georgieva, A. J. A. Aquino, F. Plasser, N. Trendafilova, A. Köhn, and H. Lischka, J. Phys. Chem. A **119**, 6232 (2015).

[22]T. Yoshihara, V. A. Galievsky, S. I. Druzhinin, S. Saha, and K. A. Zachariasse, Photochem. Photobiol. Sci. **2**, 342 (2003).

[23]P.-F. Loos, M. Comin, X. Blase, and D. Jacquemin, J. Chem. Theory Comput. **17**, 3666 (2021).

[24]M. J. G. Peach, P. Benfield, T. Helgaker, and D. J. Tozer, J. Chem. Phys. **128**, 044118 (2008).

[25]M. J. G. Peach and D. J. Tozer, J. Phys. Chem. A **116**, 9783 (2012).

[26]X. Gui, C. Holzer, and W. Klopper, J. Chem. Theory Comput. **14**, 2127 (2018).

[27]M. Casanova-Páez, M. B. Dardis, and L. Goerigk, J. Chem. Theory Comput. **15**, 4735 (2019).

[28]P. Wiggins, J. A. G. Williams, and D. J. Tozer, J. Chem. Phys. **131**, 091101 (2009).

[29]I. Knysh, I. Duchemin, X. Blase, and D. Jacquemin, J. Chem. Phys. **157**, 194102 (2022).

[30]E. E. Salpeter and H. A. Bethe, Phys. Rev. **84**, 1232 (1951).

[31]G. Csanak, H. Taylor, and R. Yaris, in *Advances in Atomic and Molecular Physics*, Advances in Atomic and Molecular Physics, Vol. 7, edited by D. Bates and I. Esterman (Academic Press, 1971) pp. 287–361.

[32]W. Hanke and L. J. Sham, Phys. Rev. Lett. **43**, 387 (1979).

[33]G. Strinati, Riv. del Nuovo Cim. **11**, 1 (1988).

[34]M. Rohlfing and S. G. Louie, Phys. Rev. Lett. **81**, 2312 (1998).

[35]S. Albrecht, L. Reining, R. Del Sole, and G. Onida, Phys. Rev. Lett. **80**, 4510 (1998).

[36]L. X. Benedict, E. L. Shirley, and R. B. Bohn, Phys. Rev. Lett. **80**, 4514 (1998).

[37]X. Blase, I. Duchemin, D. Jacquemin, and P.-F. Loos, J. Phys. Chem. Lett. **11**, 7371 (2020), pMID: 32787315, https://doi.org/10.1021/acs.jpclett.0c01875.

[38]L. Hedin, Phys. Rev. **139**, A796 (1965).

[39]M. S. Hybertsen and S. G. Louie, Phys. Rev. B **34**, 5390 (1986).

[40]R. W. Godby, M. Schlüter, and L. J. Sham, Phys. Rev. B **37**, 10159 (1988).

[41]D. Golze, M. Dvorak, and P. Rinke, Front. Chem. **7**, 377 (2019).

[42]I. Duchemin, T. Deutsch, and X. Blase, Phys. Rev. Lett. **109**, 167801 (2012).

[43]B. Baumeier, D. Andrienko, and M. Rohlfing, J. Chem. Theory Comput. **8**, 2790 (2012).

[44]P. Cudazzo, M. Gatti, A. Rubio, and F. Sottile, Phys. Rev. B **88**, 195152 (2013).

[45]V. Ziaei and T. Bredow, J. Chem. Phys. **145**, 174305 (2016).

[46]D. Jacquemin, I. Duchemin, and X. Blase, J. Phys. Chem. Lett. **8**, 1524 (2017).

[47]X. Blase, I. Duchemin, and D. Jacquemin, Chem. Soc. Rev. **47**, 1022 (2018).

[48]X. Gui, C. Holzer, and W. Klopper, J. Chem. Theory Comput. **14**, 2127 (2018), pMID: 29499116, https://doi.org/10.1021/acs.jctc.8b00014.

[49]F. Kaplan, M. E. Harding, C. Seiler, F. Weigend, F. Evers, and M. J. van Setten, J. Chem. Theory Comput. **12**, 2528 (2016).

[50]T. Rangel, S. M. Hamed, F. Bruneval, and J. B. Neaton, J. Chem. Theory Comput. **12**, 2834 (2016).

[51]D. Jacquemin, I. Duchemin, and X. Blase, J. Chem. Theory Comput. **11**, 3290 (2015).

[52]N. C. Handy and H. F. Schaefer, J. Chem. Phys. **81**, 5031 (1984).

[53]C. van Caillie and R. D. Amos, Chem. Phys. Lett. **317**, 159 (2000).

[54]F. Furche and R. Ahlrichs, J. Chem. Phys. **117**, 7433 (2002).

[55]M. S. Kaczmarski, Y. Ma, and M. Rohlfing, Phys. Rev. B **81**, 115433 (2010).

[56]S. Ismail-Beigi and S. G. Louie, Phys. Rev. Lett. **90**, 076401 (2003).

[57]M. S. Kaczmarski and M. Rohlfing, J. Phys. B: At. Mol. Opt. Phys. **43**, 051001 (2010).

[58]O. Çaylak and B. Baumeier, J. Chem. Theory Comput. **17**, 879 (2021).

[59]M. J. Frisch, G. W. Trucks, H. B. Schlegel, G. E. Scuseria, M. A. Robb, J. R. Cheeseman, G. Scalmani, V. Barone, G. A. Petersson, H. Nakatsuji, X. Li, M. Caricato, A. V. Marenich, J. Bloino, B. G. Janesko, R. Gomperts, B. Mennucci, H. P. Hratchian, J. V. Ortiz, A. F. Izmaylov, J. L. Sonnenberg, D. Williams-Young, F. Ding, F. Lipparini, F. Egidi, J. Goings, B. Peng, A. Petrone, T. Henderson, D. Ranasinghe, V. G. Zakrzewski, J. Gao, N. Rega, G. Zheng, W. Liang, M. Hada, M. Ehara, K. Toyota, R. Fukuda, J. Hasegawa, M. Ishida, T. Nakajima, Y. Honda, O. Kitao, H. Nakai, T. Vreven, K. Throssell, J. A. Montgomery, Jr., J. E. Peralta, F. Ogliaro, M. J. Bearpark, J. J. Heyd, E. N. Brothers, K. N. Kudin, V. N. Staroverov, T. A. Keith, R. Kobayashi, J. Normand, K. Raghavachari, A. P. Rendell, J. C. Burant, S. S. Iyengar, J. Tomasi, M. Cossi, J. M. Millam, M. Klene, C. Adamo, R. Cammi, J. W. Ochterski, R. L. Martin, K. Morokuma, O. Farkas, J. B. Foresman, and D. J. Fox, "Gaussian~16 Revision C.01," (2019), gaussian Inc. Wallingford CT.

[60]O. Christiansen, H. Koch, and P. Jørgensen, Chem. Phys. Lett. **243**, 409 (1995).

[61]C. Hättig and F. Weigend, J. Chem. Phys. **113**, 5154 (2000).

[62]C. Hättig, J. Chem. Phys. **118**, 7751 (2003).

[63]A. Köhn and C. Hättig, J. Chem. Phys. **119**, 5021 (2003).

[64]"TURBOMOLE V7.5.1 2021, a development of University of Karlsruhe and Forschungszentrum Karlsruhe GmbH, 1989-2007, TURBOMOLE GmbH, since 2007; available from `https://www.turbomole.org`.".

[65]G. D. Purvis and R. J. Bartlett, J. Chem. Phys. **76**, 1910 (1982).

[66]G. E. Scuseria, A. C. Scheiner, T. J. Lee, J. E. Rice, and H. F. Schaefer, J. Chem. Phys. **86**, 2881 (1987).

[67]H. Koch, H. J. A. Jensen, P. Jørgensen, and T. Helgaker, J. Chem. Phys. **93**, 3345 (1990).

[68]J. F. Stanton and R. J. Bartlett, J. Chem. Phys. **98**, 7029 (1993).

[69]J. F. Stanton, J. Chem. Phys. **99**, 8840 (1993).

[70]D. A. Matthews and J. F. Stanton, J. Chem. Phys. **145**, 124102 (2016).

[71]J. F. Stanton, J. Gauss, L. Cheng, M. E. Harding, D. A. Matthews, and P. G. Szalay, "CFOUR, Coupled-Cluster techniques for Computational Chemistry, a quantum-chemical program package," With contributions from A.A. Auer, A. Asthana, R.J. Bartlett, U. Benedikt, C. Berger, D.E. Bernholdt, S. Blaschke, Y. J. Bomble, S. Burger, O. Christiansen, D. Datta, F. Engel, R. Faber, J. Greiner, M. Heckert, O. Heun, M. Hilgenberg, C. Huber, T.-C. Jagau, D. Jonsson, J. Jusélius, T. Kirsch, K. Klein, G.M. Kopper, W.J. Lauderdale, F. Lipparini, J. Liu, T. Metzroth, L.A. Mück,

D.P. O'Neill, T. Nottoli, D.R. Price, E. Prochnow, C. Puzzarini, K. Ruud, F. Schiffmann, W. Schwalbach, C. Simmons, S. Stopkowicz, A. Tajti, J. Vázquez, F. Wang, J.D. Watts and the integral packages MOLECULE (J. Almlöf and P.R. Taylor), PROPS (P.R. Taylor), ABACUS (T. Helgaker, H.J. Aa. Jensen, P. Jørgensen, and J. Olsen), and ECP routines by A. V. Mitin and C. van Wüllen. For the current version, see http://www.cfour.de.

[72]M. Véril, A. Scemama, M. Caffarel, F. Lipparini, M. Boggio-Pasqua, D. Jacquemin, and P.-F. Loos, WIREs Comput. Mol. Sci. **11**, e1517 (2021).

[73]J. P. Perdew, K. Burke, and M. Ernzerhof, Phys. Rev. Lett. **78**, 1396 (1997).

[74]C. Adamo and V. Barone, J. Chem. Phys. **110**, 6158 (1999).

[75]T. Yanai, D. P. Tew, and N. C. Handy, Chem. Phys. Lett. **393**, 51 (2004).

[76]I. Duchemin and X. Blase, J. Chem. Theory Comput. **16**, 1742 (2020).

[77]I. Duchemin and X. Blase, J. Chem. Theory Comput. **17**, 2383 (2021), pMID: 33797245, https://doi.org/10.1021/acs.jctc.1c00101.

[78]D. Amblard, G. D'Avino, I. Duchemin, and X. Blase, Phys. Rev. Mater. **6**, 064008 (2022).

[79]D. Jacquemin, I. Duchemin, and X. Blase, J. Phys. Chem. Lett. **8**, 1524 (2017), pMID: 28301726, https://doi.org/10.1021/acs.jpclett.7b00381.

[80]J. Li, G. D'Avino, I. Duchemin, D. Beljonne, and X. Blase, J. Phys. Chem. Lett. **7**, 2814 (2016), pMID: 27388926, https://doi.org/10.1021/acs.jpclett.6b01302.

[81]F. Neese, WIREs Comput. Mol. Sci. , e1606 (2022).

[82]X. Ren, P. Rinke, V. Blum, J. Wieferink, A. Tkatchenko, A. Sanfilippo, K. Reuter, and M. Scheffler, New J. Phys. **14**, 053020 (2012).

[83]F. Neese, WIREs Comput. Mol. Sci. **2**, 73 (2012).

[84]F. Neese, F. Wennmohs, U. Becker, and C. Riplinger, J. Chem. Phys. **152**, 224108 (2020).

[85]T. Le Bahers, C. Adamo, and I. Ciofini, J. Chem. Theory Comput. **7**, 2498 (2011).

[86]D. Jacquemin, T. L. Bahers, C. Adamo, and I. Ciofini, Phys. Chem. Chem. Phys. **14**, 5383 (2012).

[87]M. Schreiber, M. R. Silva-Junior, S. P. A. Sauer, and W. Thiel, J. Chem. Phys. **128**, 134110 (2008).

[88]D. Kánnár and P. G. Szalay, J. Chem. Theory Comput. **10**, 3757 (2014).

[89]A. D. Laurent and D. Jacquemin, Int. J. Quantum Chem. **113**, 2019 (2013).

[90]D. Jacquemin, I. Duchemin, A. Blondel, and X. Blase, J. Chem. Theory Comput. **12**, 3969 (2016), http://dx.doi.org/10.1021/acs.jctc.6b00419.

[91]C. A. McKeon, S. M. Hamed, F. Bruneval, and J. B. Neaton, J. Chem. Phys. **157**, 074103 (2022), https://doi.org/10.1063/5.0097582.